0026-895X/01/5902-193–202$3.00
MOLECULAR PHARMACOLOGY
Copyright © 2001 The American Society for Pharmacology and Experimental Therapeutics
Mol Pharmacol 59:193–202, 2001

Vol. 59, No. 2
311/877515
Printed in U.S.A.

Nitrogen-Bisphosphonates Block Retinoblastoma Phosphorylation and Cell Growth by Inhibiting the Cholesterol Biosynthetic Pathway in a Keratinocyte Model for Esophageal Irritation

ALFRED A. RESZKA, JUDIT HALASY-NAGY, and GIDEON A. RODAN

Department of Bone Biology and Osteoporosis Research, Merck Research Laboratories, West Point, Pennsylvania

Received August 24, 2000; accepted October 6, 2000

This paper is available online at http://molpharm.aspetjournals.org

ABSTRACT

The surprising discovery that nitrogen-containing bisphosphonates (N-BPs) act via inhibition of the mevalonate-to-cholesterol pathway raised the possibility that esophageal irritation by N-BPs is mechanism-based. We used normal human epidermal keratinocytes (NHEKs) to model N-BP effects on stratified squamous epithelium of the esophagus. The N-BPs alendronate and risedronate inhibited NHEK growth in a dose-dependent manner without inducing apoptosis. N-BPs (30 μM) caused accumulation of cells in S phase and increased binucleation (inhibited cytokinesis). Consistent with N-BP inhibition of isoprenylation, geranylgeraniol or farnesol prevented accumulation in S phase. Binucleation was also induced by the 3-hydroxy-3-methylglutaryl-coenzyme A reductase inhibitor lovastatin and by the squalene synthase inhibitor zaragozic acid A and was prevented by adding low-density lipoprotein. At 300 μM, N-BPs reduced expression of cyclin-dependent kinase (cdk) 2 and cdk4 and enhanced expression of $p21^{waf1}$ and $p27^{kip1}$ and their binding to cdks with corollary hypophosphorylation of retinoblastoma. Lovastatin and zaragozic acid A produced similar effects, except that $p21^{waf1}$ expression and binding to cdks was not induced. Growth inhibition, but not binucleation, was also caused by the geranylgeranyl transferase I inhibitor, GGTI-298, which also enhanced cdk2 and cdk4 association with $p27^{kip1}$. These findings are consistent with suppression of epithelial cell growth by N-BPs via inhibition of the mevalonate pathway and the consequent reduction in cholesterol synthesis, which blocks cytokinesis, and in geranylgeranylation, which interferes with progression through the cell cycle.

Skin and esophagus are covered by stratified squamous epithelium, which provides a protective barrier for the underlying tissues. Inhibition of 3-hydroxy-3-methylglutaryl-coenzyme A (HMG-CoA) reductase by statins applied topically can lead to barrier disruption (Feingold et al., 1990, 1991; Menon et al., 1992), which correlates with a low incidence of skin irritation observed in clinical practice (Tobert, 1988). Bisphosphonates (BPs) are widely used for the prevention and treatment of osteoporosis and other bone diseases. BPs are targeted to bone and after oral administration have only a brief presence in serum, but can cause a low incidence of esophageal irritation, associated with acid reflux and improper dosing (de Groen et al., 1996). Various studies have examined BP-induced upper gastrointestinal irritation in vivo (Blank et al., 1997; Elliott et al., 1998; Peter et al., 1998a,b; Wallace et al., 1999). At very high doses, topical but not systemic BP administration can induce gastric lesions in rodents (Elliott et al., 1998). At clinically relevant doses, esophageal irritation can be elicited in dogs with topical administration of BPs in the presence of simulated gastric juice (pH 2.0) or after prior exposure of the esophagus to acid (Peter et al., 1998a). BP potency is related to the side chain attached to the geminal carbon in the P-C-P backbone. Similar rank order potency for BP gastrointestinal effects (Peter et al., 1998a,b) and for clinical efficacy suggest that gastrointestinal effects could be mechanism-based. However, at very high doses (300- to 900-fold above clinical dosing), nitrogen-containing bisphosphonates (N-BPs) were shown to cause various degrees of gastric irritation when administered to rodents for short periods of time in the presence of indomethacin (Blank et al., 1997; Elliott et al., 1998). Rat gastric epithelial necrosis was also observed within 30 min of appli-

ABBREVIATIONS: HMG, 3-hydroxy-3-methylglutaryl; CoA, coenzyme A; BP, bisphosphonate; N-BP, nitrogen-containing bisphosphonate; ALN, alendronate; RIS, risedronate; FPP, farnesyl diphosphate; NHEK, normal human epidermal keratinocyte; pRb, retinoblastoma; LOV, lovastatin; ANOVA, analysis of variance; FACS, fluorescence-activated cell sorting; HBS, HEPES-buffered saline; cdk, cyclin-dependent kinase; Zara-A, zaragozic acid A; GGTI, geranylgeranyl transferase; FTI, farnesyl transferase; FTI-1, 5(*S*)-*n*-butyl-4-[1-(4-cyanobenzyl)imidazol-5-ylmethyl]-1-(3-trifluoromethoxyphenyl)piperazin-2-one; LDL, low-density lipoprotein; GGOH, geranylgeraniol; FOH, farnesol.

cation of N-BP in the absence of indomethacin at doses ≥200-fold, but not ≤100-fold, above clinical oral dosing (Wallace et al., 1999). This leaves open the question of whether the N-BPs cause irritation via chemical toxicity or through the same mechanism by which bone resorption is suppressed (i.e., inhibition of the mevalonate pathway).

N-BPs [e.g., alendronate (ALN), pamidronate, risedronate (RIS), ibandronate, and olpadronate] contain a side-chain nitrogen that is separated from the geminal carbon by two or three carbon atoms. These, but not BPs lacking nitrogen, act via inhibition of farnesyl diphosphate (FPP) synthase in the mevalonate to cholesterol pathway (Amin et al., 1992; Luckman et al., 1998; Benford et al., 1999; Fisher et al., 1999; Reszka et al., 1999, van Beek et al., 1999a,b; Bergstrom et al., 2000). In this regard, the presence of a nitrogen atom in the BP seems sufficient to confer inhibitory action, without regard to whether it is in the form of a primary, secondary (pyridinyl), or tertiary amine. Although inhibition of FPP synthase or HMG-CoA reductase blocks, among others, cholesterol biosynthesis and protein isoprenylation (farnesylation and two types of geranylgeranylation), only geranylgeranylation seems to be rate-limiting for inhibition of bone resorption (Fisher et al., 1999; van Beek et al., 1999a). N-BP induction of apoptosis in osteoclasts and other cells is also caused by inhibition of protein isoprenylation (Luckman et al., 1998; Shipman et al., 1998; Benford et al., 1999; Reszka et al., 1999), required for the function of such key regulatory proteins as Ras, Rac, Rho, cdc42 etc.

To examine whether N-BP gastrointestinal effects are based on inhibition of FPP synthase, we studied the effects of ALN and RIS, dosed at clinically-relevant concentrations (≤ 300 μM), on normal human epidermal keratinocytes (NHEKs), a model system for stratum basale of the stratified squamous epithelium that covers both skin and the esophagus. Contrary to previous observations in osteoclasts, and other cells (Hughes et al., 1995; Luckman et al., 1998; Shipman et al., 1998; Benford et al., 1999; Reszka et al., 1999), ALN and RIS did not induce apoptosis but instead inhibited proliferation in a dose-dependent manner. This effect correlated with the complete block of retinoblastoma (pRb) phosphorylation at 300 μM, where full growth arrest was observed. Growth inhibition was prevented by addition of downstream metabolites and, in most regards, mimicked by the HMG-CoA reductase inhibitor, lovastatin (LOV). ALN and RIS induced expression of both $p21^{waf1}$ and $p27^{kip1}$ and enhanced their binding to cdks 2 and 4. An analysis of N-BP effects on growth, cell cycle markers and protein isoprenylation in NHEKs is presented in this study.

Materials and Methods

Keratinocyte Proliferation. NHEKs (Clonetics, Walkersville, MD), seeded at 5000/well in CytoStar scintillating microplates (Amersham Pharmacia Biotech Inc., Piscataway, NJ), were grown in keratinocyte growth medium (KGM; Clonetics) for 24 h. Media were then changed and [^{14}C]thymidine (NEN, Boston, MA) was added at 0.5 μCi/ml along with indicated pharmacological agents (all synthesized or purified at Merck and Co., Inc., West Point, PA), tested in triplicate. Radioactivity incorporated at 37°C was measured at 24-h intervals for 3 days using a TopCount NTX microplate scintillation counter (Packard, Meriden, CT). Results were analyzed using ANOVA factorial method (SAS Institute Inc., Cary, NC).

NHEK Binucleation Assay. NHEKs (20,000/well) were grown in 24-well plates in KGM for 24 h, after which indicated (legend to Fig. 3) (duplicate) treatments lasted 48 h. Cells were then fixed in 10% formaldehyde in PBS. Nuclei were stained with Hoechst 33342 (Sigma, St. Louis, MO) (5 μg/ml in PBS with 0.1% Triton X-100) for 10 min. Cells were counter-stained with Eosin Y (1%) for 5 min, then mounted using SlowFade Light mounting medium (Molecular Probes, Eugene, OR). Three microscopic fields of each well were photographed under phase contrast and then ultraviolet illumination. Binucleation was quantified in phase contrast photographs and verified by comparison with UV images. Results were analyzed using ANOVA.

Cell Cycle/DNA Fluorescence-Activated Cell Sorting (FACS) Analysis. NHEKs were seeded (100,000 cells/6 cm dish) in KGM and grown 24 h. Treatments lasted 48 h to allow depletion of intracellular pools of isoprenoids and subsequent growth arrest. Cells were released with trypsin/EDTA (Clonetics) and then fixed in 70% ethanol at −20°C overnight. It is notable that NHEKs treated 72 h with ALN or RIS adhered tightly to the tissue culture plastic and could not be detached with trypsin/EDTA for analysis (data not shown). Fixed cells were treated with Rnase A (100 μg/ml in H_2O; Boehringer Mannheim, Germany) for 5 min at room temperature, and then propidium iodide (50 μg/ml; Sigma, St. Louis, MO) was added for an additional ≥30 min at room temperature. Cells (20,000 cells/group) were sorted by FACS (FACSCalibur; Becton Dickenson, San Jose, CA), using 488 nm excitation, recording emitted fluorescence at >620 nm. Triplicate data were analyzed by ModFit LT (Verity Software House Inc., Topsham, ME) and ANOVA.

Immunoprecipitation and Immunoblot Analyses. NHEKs (20–25% confluence) were grown for 24 to 48 h in KGM. Cells were then treated with indicated compounds for indicated times. Cells were then washed twice with HBS (at 4°C): 50 mM HEPES, pH 7.6, 1 mM NaF, 150 mM NaCl, 1 mM EGTA, and then lysed in HBS supplemented with 1 μM Microcystin LR, 1 mM Na_3VO_4, 1 μM dithiothreitol, 20 μg/ml 1,10-phenanthrolene, 0.1% Triton X-100, and 1 % protease inhibitor cocktail (Sigma) with the following final concentrations: 240 μg/ml 4-(2-aminoethyl)-benzenesulfonyl fluoride, 5 μg/ml epoxysuccinyl-L-leucylamido (4-guanido)butane, 14 μg/ml bestatin, 10.5 μg/ml leupeptin, 5 μg/ml aprotinin, and 10.5 μg/ml pepstatin A. Lysates were sonicated in an ice water bath for 20 min, and insoluble material was pelleted by microcentrifugation. For analysis of crude lysates, samples were boiled in Laemmli sample buffer (Bio-Rad) supplemented with 5% β-mercaptoethanol and the above protease inhibitor cocktail at a 10-fold higher concentration. For immunoprecipitations, 250 to 400 μg of lysate were suspended in 1 ml of HBS-Tween buffer (HBS lysis buffer with 0.05% Tween 20 substituted for Triton X-100). Anti-cdk2 (goat), -cdk4 (goat), or Rap1 (rabbit) polyclonal antibodies (Santa Cruz Biotechnology, Santa Cruz, CA) were added at 3 to 4 μg/ml, along with Protein G- (goat) or A- (rabbit) conjugated agarose (Sigma). After mixing overnight at 4°C, immunoprecipitates were washed twice with HBS-Tween buffer before boiling. Immunoblot analyses were performed using standard techniques. The following antibodies were used as probes: anti-pRb, -p21 (both mouse), and -cdk4 (rat) monoclonal (Pharmingen, San Diego, CA); anti-cdk2 and -p53 (mouse) monoclonal, anti-$p57^{skp2}$ and -Rap1A (goat) polyclonal, and anti-Rap1 (rabbit) polyclonal (Santa Cruz Biotechnology); anti-Ras and anti-$p27^{skp1}$ (mouse) monoclonal (Transduction Laboratories, San Diego, CA); and anti-hDNAJ (mouse) monoclonal (NeoMarkers, Union City, CA). Antibodies were diluted 1:1000 in Tris-buffered saline/Tween: 10 mM Tris-HCl, pH 7.6, 150 mM NaCl, 0.05% Tween 20, supplemented with 0.1% (w/v) bovine serum albumin, and 0.02% NaN_3. Alkaline-phosphatase-conjugated secondary anti-mouse, -rat, -goat, or -rabbit antibodies were used at 1:10,000. After washing, blots were developed using a STORM860 (Molecular Dynamics, Hercules, CA).

Results

N-BPs and Inhibitors of Cholesterol Biosynthesis and of Isoprenylation Inhibit Keratinocyte Growth. Using primary NHEK cultures as a model for the stratified squamous epithelium that lines the esophagus, we found that in contrast to N-BP effects on osteoclasts, ALN or RIS (10–300 μM) did not cause apoptosis, cell detachment, or activation of stress-responsive kinases (data not shown). Instead, N-BPs dose dependently inhibited cell proliferation, measured by [^{14}C]thymidine incorporation (Fig. 1 A and B) and cell number or protein mass (data not shown). Significant inhibition of NHEK growth was observed at 30 μM ALN (47% of control) or 10 μM RIS (59% of control), with complete inhibition at 100 to 300 μM; these concentrations are comparable with those reached in the stomach (or during esophageal reflux) at clinical dosing (150–300 μM at 5–10 mg oral dose). Effects on cell growth were reversed by removal of bisphosphonate (data not shown).

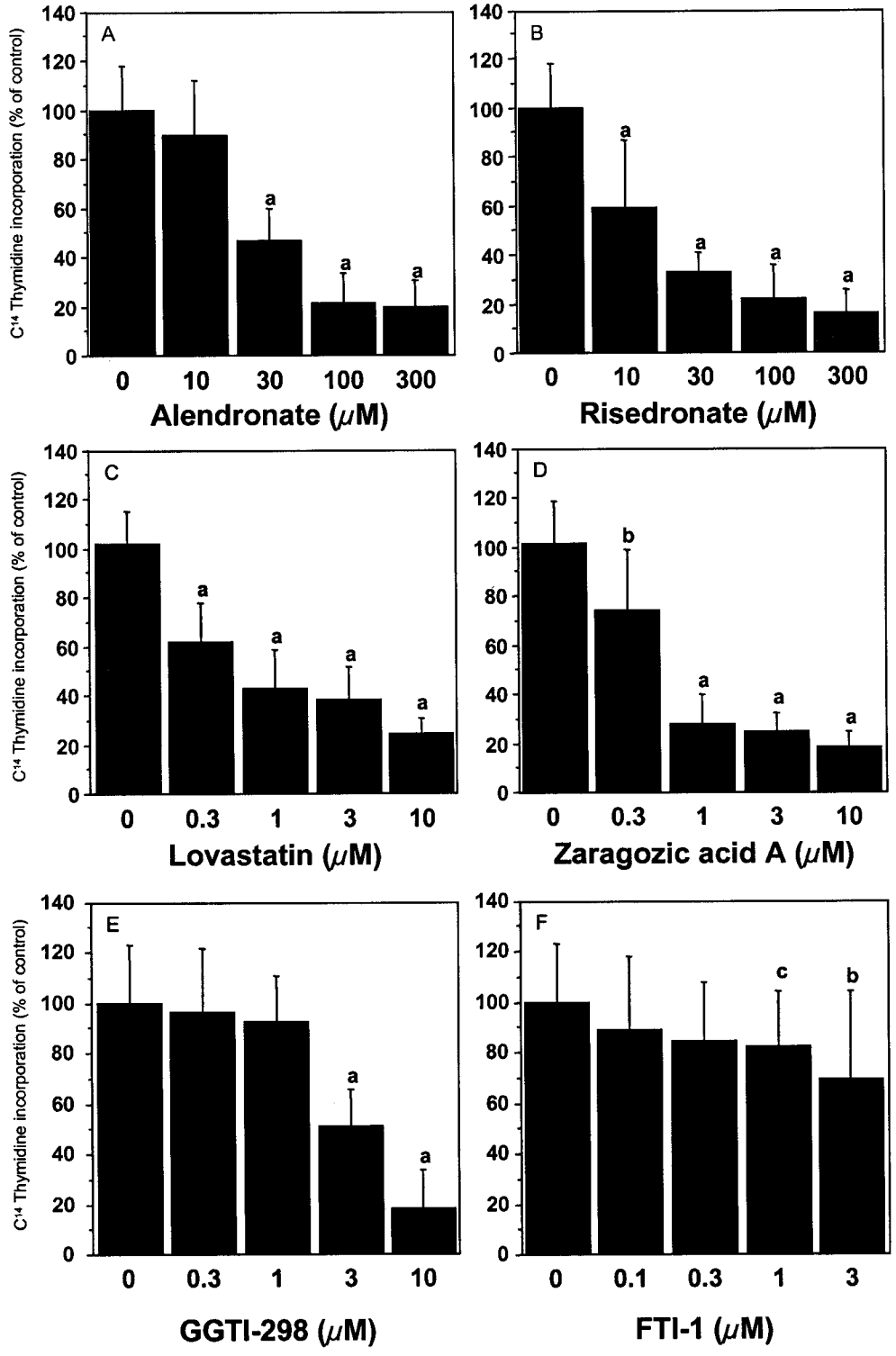

Fig. 1. Dose-dependent N-BP inhibition of NHEK growth and comparison with other mevalonate pathway and isoprenylation inhibitors. NHEKs were seeded into 96-well scintillating microplates and growth was assessed after 72 h incubation with the following: ALN (A); RIS (B); LOV (C); Zara-A (D); GGTI-298 (E); and FTI-1 (F) as described under *Materials and Methods*. Concentrations of each pharmacological agent are indicated on the *x*-axis and [^{14}C]thymidine (% of control) incorporation as a measure of cell growth is plotted on the *y*-axis. Data are presented as mean ± S.D. (n = 3 triplicate experiments). Statistical significance versus control: $^{a}p < 0.0001$; $^{b}p < 0.002$; $^{c}p < 0.05$.

To examine whether inhibition of the mevalonate pathway suppresses NHEK growth, the cells were treated with the HMG-CoA reductase inhibitor LOV (Fig. 1C). LOV dose-dependently inhibited NHEK growth starting at 0.3 μM (47% of control). The squalene synthase inhibitor zaragozic acid A (Zara-A; Fig. 1D), the geranylgeranylation inhibitor GGTI-298 (McGuire et al., 1996; Fig. 1E), and a potent and selective farnesyl transferase inhibitor FTI-1 (Williams et al., 1999; Fig. 1F) were used to investigate the relative contributions of the three branch pathways downstream of FPP synthase. The effects of Zara-A (28% of control at 1 μM) and GGTI-298 (51% of control at 3 μM) were more pronounced than those of the FTI-1 inhibitor (69% of control at 3 μM), which was effective only well above the farnesyl transferase inhibitory concentrations (see below). At 10 μM, GGTI-298 inhibition of growth was maximal (18% of control) but also caused accumulation of nonadherent, potentially apoptotic cells (data not shown). Significant cell detachment was not observed with any other treatment.

N-BPs Inhibit Protein Isoprenylation in NHEKs. The absence of cell detachment, of apoptosis, or of necrosis suggested that chemical toxicity did not occur at growth inhibitory doses of N-BP. We therefore examined whether the dose of N-BP necessary to inhibit geranylgeranylation in NHEKs (Fig. 2A) was comparable with that required for growth inhibition (Fig. 1). To detect inhibition of geranylgeranylation, we used an anti-Rap1A antibody that preferentially binds to the nongeranylgeranylated, slower migrating form of this small GTPase (Fig. 2, A and B). A nonselective anti-Rap1 antibody used to probe crude lysates (Fig. 2B, left) detected both the faster-migrating prenylated Rap1 band in control and the slower-migrating nongeranylgeranylated band (caused by the retention of three C-terminal amino acid residues normally cleaved after isoprenylation) in response to treatment with ALN, RIS,

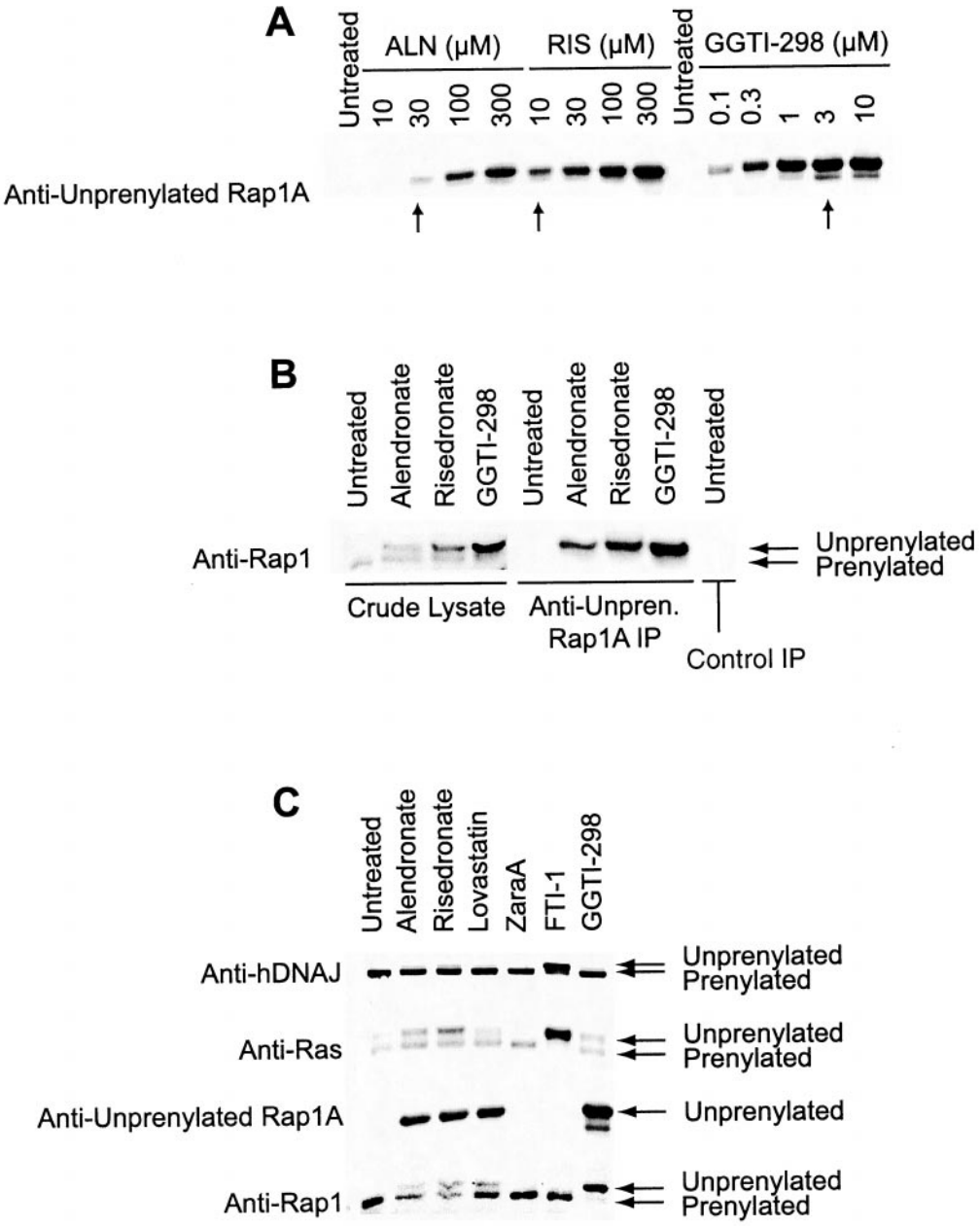

Fig. 2. Effects of N-BPs and other mevalonate pathway and isoprenylation inhibitors on geranylgeranylation and farnesylation. NHEKS were grown with indicated compounds at indicated concentrations for 24 h (A and B) or 72 h (C) and then isoprenylation markers were examined by immunoblot analysis as described under *Materials and Methods*. Rap1 geranylgeranylation. A, anti-(unprenylated) Rap1A immunoblot of crude lysates from untreated NHEKs and NHEKs treated with ALN, RIS, or GGTI-298 at indicated concentrations. B, anti-Rap1 immunoblot of crude lysates and anti-(unprenylated) Rap1A immunoprecipitates with indicated treatments. Lanes were loaded with crude lysate (10 μg) or immunoprecipitates (from 100 μg of lysate) from untreated NHEKs or NHEKs treated with ALN (300 μM), RIS (300 μM), or GGTI-298 (3 μM). Note that whereas anti-Rap1 recognizes in crude lysates both geranylgeranylated Rap1 (faster migrating band) and ungeranylgeranylated Rap1 (slower migrating band), anti-Rap1A immunoprecipitates only the unprenylated form. C, anti-hDNAJ and anti-Ras (farnesylation markers), along with anti-unprenylated Rap1A and anti-Rap1 (geranylgeranylation markers) were used, as indicated to the left of each panel, to probe immunoblots of crude lysates of untreated NHEKs and NHEKs treated as follows: ALN (300 μM), RIS (300 μM), LOV (3 μM), Zara-A (3 μM), FTI-1 (0.3 μM), and GGTI-298 (3 μM). For anti-hDNAJ, -Ras, and -Rap1 immunoblots, the unprenylated form of each respective protein migrates more slowly than the fully processed form as indicated to the right of each panel. Note that the band-shift for hDNAJ (50 kDa) is more subtle than for Ras (21 kDa). Data are representative of ≥4 experiments.

or GGTI-298. Immunoprecipitation with the preferential anti-Rap1A antibody resulted in purification of only the slower-migrating (nongeranylgeranylated) band, detected by the non-selective antibody in immunoblot analyses (Fig. 2B, right). Probing crude lysates with the antibody against nongeranylgeranylated Rap1A proved to be the most sensitive method for detecting N-BP effects (Fig. 2A). ALN and RIS dose dependently inhibited geranylgeranylation, starting at 30 μM and 10 μM, respectively (Fig. 2A), concentrations identical to those that inhibited growth (arrows in Fig. 2A point to lowest concentrations that inhibited growth). GGTI-298 inhibited Rap1A geranylgeranylation with an IC_{50} value between 0.3 and 1 μM (Fig. 2A) compared with the IC_{50} for growth inhibition of 3 μM, where geranylgeranylation was maximally inhibited.

Farnesylation was measured by examining the heat shock protein hDNAJ, and the small GTPase, Ras (Fig. 2C). As noted above, the nonfarnesylated forms of these proteins show reduced migration during electrophoresis. Farnesylation was inhibited by ALN and RIS, affecting Ras more extensively than hDNAJ. To test whether the different degree of farnesylation inhibition could be caused by turnover or specific pools of these proteins, we also examined the effects of LOV (3 μM), FTI-1 (0.3 μM), and GGTI-298 (3 μM) (Fig. 2C) on isoprenylation. FTI-1 at 0.3 μM completely inhibited farnesylation of both hDNAJ and Ras, showing that protein turnover was sufficient to generate a sizable pool of unprenylated protein. GGTI-298 was not as selective as FTI-1 and modestly inhibited farnesylation of hDNAJ and Ras at the growth-inhibitory concentration of 3 μM. Mixtures of FTI-1 and GGTI-298 at several doses did not alter the growth response to GGTI-298 (data not shown). As predicted, Zara-A (3 μM) did not affect isoprenylation of any marker.

Surprisingly, although LOV inhibited Rap1A geranylgeranylation to the same extent as ALN and RIS (Fig. 2C, bottom), it had little effect on either hDNAJ or Ras farnesylation. Indeed, the rank order of selectivity for inhibition of farnesylation was FTI-1 $\ggg$ RIS = ALN > GGTI-298 $\geq$ LOV, whereas selectivity for inhibition of geranylgeranylation was GGTI-298 $\geq$ LOV > ALN = RIS with FTI-1 inactive. These findings confirm the pharmacological activity of these agents on protein isoprenylation and suggest preference of LOV for inhibition of geranylgeranylation, via mechanism(s) which require further study.

N-BPs Inhibition of Cholesterol Biosynthesis Induces NHEK Binucleation. Phase-contrast microscopy, verified by Hoechst nuclear staining, showed that 1.8% of cells in untreated controls were binucleated (Fig. 3A, arrows). The fraction of binucleated cells increased to 11.3% in cells treated with 1 μM LOV (Fig. 3B), to 8.4% with 30 μM RIS (Fig. 3C), to 7.3% with 30 μM ALN (Fig. 3E), and to 10.6% with1 μM Zara-A (Fig. 3G). This 4- to 6-fold increase in binucleation ($p < 0.0001$ versus control for each treatment) suggests that these agents blocked cytokinesis. Nonsignificant accumulation of binucleated cells (versus control) was observed after treatment with GGTI-298 (4.1% at 3 μM; Fig. 3F) or N-BPs at 300 μM (data not shown), possibly because of arrest in G_1 by the latter (see below).

Because only the agents that inhibited cholesterol synthesis induced binucleation, we added low-density lipoprotein (LDL; 500 μg/ml) as a source of cholesterol to the medium (which otherwise lacks lipoprotein) of cells treated with either ALN (30 μM, Fig. 3F) or Zara-A (1 μM, Fig. 3H) in an attempt to rescue this phenotype. In two of five experiments, LDL seemed toxic to the cells (data not shown); in the remaining three experiments, however, LDL blocked accumulation of binucleated cells induced by 30 μM ALN (3.2% binucleated, $p < 0.003$ versus ALN, not significant versus control) or by 1 μM Zara-A (3.6% binucleated, $p < 0.0001$ versus Zara-A, not significant versus control). LDL increased cell number to control levels in the presence of Zara-A, but not ALN (data not shown), most likely because of its additional inhibition of geranylgeranylation. [^{14}C]thymidine incorporation experiments with LDL and ALN confirmed these findings (not significant versus ALN; data not shown), suggesting that inhibition of cholesterol biosynthesis by either agent was sufficient to inhibit growth but could not fully

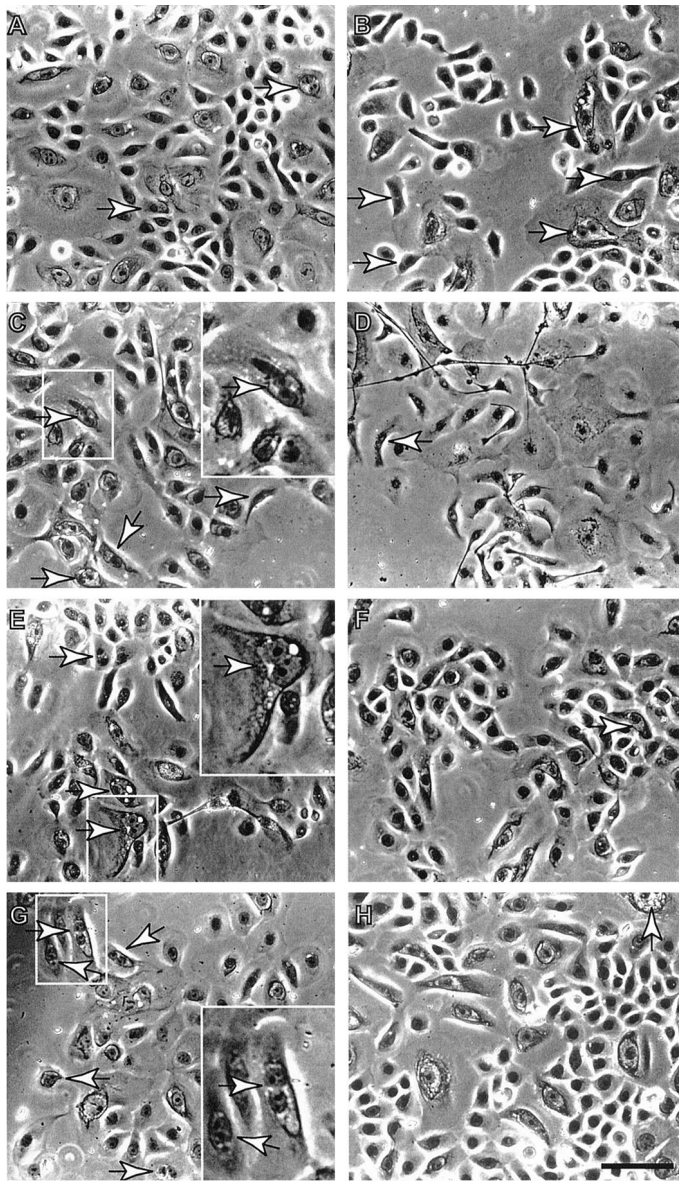

Fig. 3. Effects of N-BPs and other mevalonate pathway and isoprenylation inhibitors on binucleation of NHEKs. NHEKs were treated with compound for 48 h and then fixed, stained, and photographed as described under *Materials and Methods*. Cells were untreated (A) or treated as follows: 3 μM LOV (B); 30 μM RIS (C); 3 μM GGTI-298 (D); 30 μM ALN (E); 30 μM ALN and 500 μg/ml LDL (F); 1 μM Zara-A (G); 1 μM Zara-A and 500 μg/ml LDL (H). Arrows indicate cells with two nuclei; inset boxes are 200% magnifications of indicated regions. Bar, 200 μm.

account for the ALN effects. These findings confirm the pharmacological activity of Zara-A for inhibition of sterol synthesis in this system.

N-BP Inhibition of Isoprenylation Causes Partial Cell Cycle Arrest in S Phase. To expand analysis of N-BP effects on cell growth, FACS analysis of DNA content was used to estimate the distribution of cells in the phases of the cell cycle (Table 1 and Fig. 4). In control cultures, 63% of NHEKs had 2n (G_1/G_0) DNA content, 15% had 4n (G_2/M) DNA content, and 22% had 2n < DNA < 4n (S phase). Cells treated with either ALN or RIS showed comparable concentration-dependent shifts in DNA profile (Table 1). At 30 μM, ALN and RIS caused the largest (2.1- to 2.6-fold) increase in the number of cells in S phase, accompanied by reductions in cells in G_1/G_0 and G_2/M. Because N-BPs cause only partial growth inhibition at 30 μM, this represents a reduction in the rate of transit through S phase rather than a complete arrest. Consistent with strong effects on binucleation, LOV or Zara-A nearly doubled the number of cells in G_2/M.

At 300 μM N-BP, most cells were found to be in G_0/G_1 (Table 1). Indeed, the FACS profile was nearly indistinguishable from that of control. Because these cells were not growing, this suggests arrest in several phases of the cell cycle, the most prominent being G_0/G_1, probably because of the presence of most cells in this phase before addition of the N-BPs. NHEK populations treated with GGTI-298 showed a significant decline in cells in G_2/M with relatively little impact on G_0/G_1 or S phases. Consistent with mild effects on growth, FTI-1 did not significantly impact the FACS DNA profile.

Because replenishment of cholesterol was only partially effective in restoring cell growth inhibited by ALN, we next tested whether N-BP effects could be prevented by adding geranylgeraniol (GGOH) or farnesol (FOH), which can be converted to mevalonate pathway intermediates and prevent the reduction in isoprenylation. However, GGOH and FOH inhibit choline phosphotransferase (Miquel et al., 1998), which was rate-limiting for NHEK growth. Therefore, phosphatidylcholine was also added to each culture (40 μg/ml) and did not seem to alter the response to N-BP treatment. ALN reduced the number of cells with G_1/G_0 DNA content by 39% compared with control but increased the population of cells in S phase by 1.9-fold (Fig. 4, inset table). Addition of either GGOH or FOH increased the number of cells in G_1/G_0, and reduced the number of cells in S phase, resulting in a profile comparable with that of control (Fig. 4).

Effects of GGOH and FOH (in the presence of phosphatidylcholine) on cell proliferation inhibited by ALN (30 μM) were also examined. Figure 5 shows averaged values from two independent 72 h experiments (performed in triplicate), in which relative incorporation of [^{14}C]thymidine was increased by the addition of GGOH to ALN-treated cells from 39 to 54% at 48 h and 23 to 38% at 72 h. Addition of GGOH plus FOH further increased [^{14}C]thymidine incorporation to 65 and 50% ($p < 0.05$) at 48 and 72 h, respectively. These findings support the conclusion that ALN inhibition of growth is caused by suppression of isoprenylation. In further experiments, LDL was combined with FOH or GGOH in the absence or presence of ALN in attempts to replenish cholesterol. However LDL on its own was found to produce some toxicity and in combination with GGOH was more toxic. LDL by itself reduced [^{14}C]thymidine incorporation by 17% and with GGOH by 30%. More pronounced cytotoxicity and growth suppression in the presence of the other lipid additions thus interfered with the possibility of conducting this reconstitution experiment, resulting in thymidine incorporation below that achieved with ALN alone. In an separate triplicate experiment, neither FOH nor GGOH increased [^{14}C]thymidine incorporation inhibited by Zara-A.

Mevalonate Pathway and Geranylgeranylation Inhibitors Induce Hypophosphorylation of pRb, via Effects on Cyclin-Dependent Kinases (cdks) and Their Inhibitors. Progression through the cell cycle involves several checkpoints, regulated in part by pRb, which is under the control of cdks. GGTI-298 was previously shown to reduce, but not eliminate, phosphorylation of pRb in human tumor cells (Sun et al., 1999). N-BP effects on cell cycle regulators were studied at 300 μM, which caused most cells to arrest in G_1 where pRb acts. Treatment with ALN, RIS, LOV, and Zara-A resulted in essentially complete hypophosphorylation of pRb (Fig. 6A) and reduced its overall expression by approximately 50%. GGTI-298 caused a milder pRb hypophosphorylation than was observed with the cholesterol-blocking agents, whereas treatment with FTI-1 had little effect.

Changes in cdks, which phosphorylate pRb, and in cdk inhibitors and activators (Fig. 6A) were all consistent with the hypophosphorylation of pRb. Interestingly there was a

TABLE 1

Distribution of NHEK population in various phases of the cell cycle

NHEKs were treated for 48 hr with indicated compounds and analyzed for DNA content by FACS. Data are the mean percentage (± S.D.) of cells in G_0/G_1, S, and G_2/M phases as determined by ModFit LT software ($n = 3$).

	G_0/G_1		S		G_2/M	
	Mean	(S.D.)	Mean	(S.D.)	Mean	(S.D.)
Control	63.1	(4.2)	22.0	(2.7)	14.8	(2.0)
ALN 300 μM	56.2	(1.9)	31.8	(6.3)	12.0	(6.4)
ALN 30 μM	32.4*	(3.1)	57.3*	(1.6)	10.3	(1.6)
RIS 300 μM	56.2	(6.5)	35.4***	(4.8)	8.4***	(1.7)
RIS 30 μM	33.3*	(23)	46.8*	(7.0)	9.6***	(0.35)
Lov 1 μM	49.4***	(4.4)	25.8	(9.4)	24.8**	(5.0)
ZaraA 1 μM	54.7	(7.7)	22.6	(8.2)	22.7**	(0.58)
GGTI-298 3 μM	68.3	(12)	22.2	(9.0)	9.5***	(3.2)
FTI-1 0.3 μM	57.8	(9.8)	26.3	(10)	16.0	(1.1)

* $p \leq 0.0001$ vs. control.
** $p < 0.003$ vs. control.
*** $p < 0.05$ vs. control.

marked difference in the effects of these agents, which target different enzymes in the mevalonate pathway. ALN, RIS, LOV, or Zara-A, but not GGTI-298 or FTI-1, reduced expression of cdk2 by approximately 50% and cdk4 by up to 80%. Expression of $p19^{skp1}$, which binds cdk2 and is required for ubiquitin-mediated proteolysis of the cdk inhibitor $p21^{waf1}$ (Bai et al., 1996, Yu et al., 1999), was reduced upon treatment with ALN, RIS, LOV, Zara-A, and to a lesser extent, GGTI-298 and FTI-1. Interestingly, expression of the cdk inhibitor, $p21^{waf1}$, was increased approximately 2-fold by ALN or RIS, but not by the other treatments. Indeed, treatment with LOV or Zara-A consistently reduced $p21^{waf1}$ expression. This provided a second example of the inability of LOV to fully mimic the activity of the N-BPs. Expression of the cdk inhibitor, $p27^{kip1}$, but not $p57^{kip2}$, was increased by ALN, RIS, Zara-A, and, to a lesser extent, LOV and GGTI-298, but not by FTI-1. Interestingly, expression of p53 was reduced by up to 70% after treatment with ALN, RIS, LOV, or Zara-A, but not GGTI-298 or FTI-1 (Fig. 6A). This is consistent with N-BP inhibition of growth in the absence of NHEK apoptosis.

A second parameter that may control phosphorylation of pRb and progression through the cell cycle is the association between cdks and their inhibitors. We analyzed this interaction by coimmunoprecipitation. In pull-down experiments, association of $p21^{waf1}$ or $p27^{kip1}$ with cdk4 (Fig. 6B) and cdk2 (Fig. 6C), measured as precipitated kinase relative to coprecipitated inhibitor, was increased approximately 2- to 4-fold as follows: 1) $p21^{waf1}$ association with cdk4 (Fig. 6B) after ALN or RIS but not LOV, Zara-A, FTI-1 or GGTI-298 treatment; 2) $p27^{kip1}$ association with cdk4 (Fig. 5B) after all treatments; 3) $p21^{waf1}$ association with cdk2 (Fig. 6C) after ALN, RIS, FTI-1 or GGTI-298, but not LOV or Zara-A; and 4) $p27^{kip1}$ association with cdk2 (Fig. 6C) after all treatments, except Zara-A.

Discussion

We and others have recently shown that N-BPs inhibit the mevalonate pathway in osteoclasts (Fisher et al., 1999; Reszka et al., 1999; van Beek et al., 1999a; Bergstrom et al., 2000), thus reducing isoprenylation and cholesterol biosynthesis and causing inhibition of bone resorption and induction of osteoclast apoptosis. Geranylgeranyl diphosphate was rate-limiting for these effects. In this study, we used primary NHEK cultures as a model system to investigate possible mechanism-based effects of N-BPs, at clinically relevant concentrations, on the esophagus. The esophagus, similar to skin, is lined by stratified squamous epithelium, consisting of an upper, terminally differentiated layer (*stratum corneum*) nearest to the lumen, an adjacent differentiating layer (*stratum spinosum*) and a growing layer (*stratum basale*). *Stratum corneum* is continually replaced through growth and differentiation within the underlying strata. Cells of the *stra-*

	G0/G1		S		G2/M	
	Mean	(SD)	Mean	(SD)	Mean	(SD)
Control	54.2	(7.7)	29.6	(8.8)	16.2	(1.3)
ALN	33.2 [a]	(4.8)	57.7 [a]	(6.8)	9.1 [a]	(2.9)
ALN/FOH	55.8 [b]	(3.9)	34.8 [b]	(1.9)	9.4 [a]	(2.3)
ALN/GGOH	53.4 [b]	(4.6)	35.7 [b]	(9.3)	10.9 [a]	(4.7)

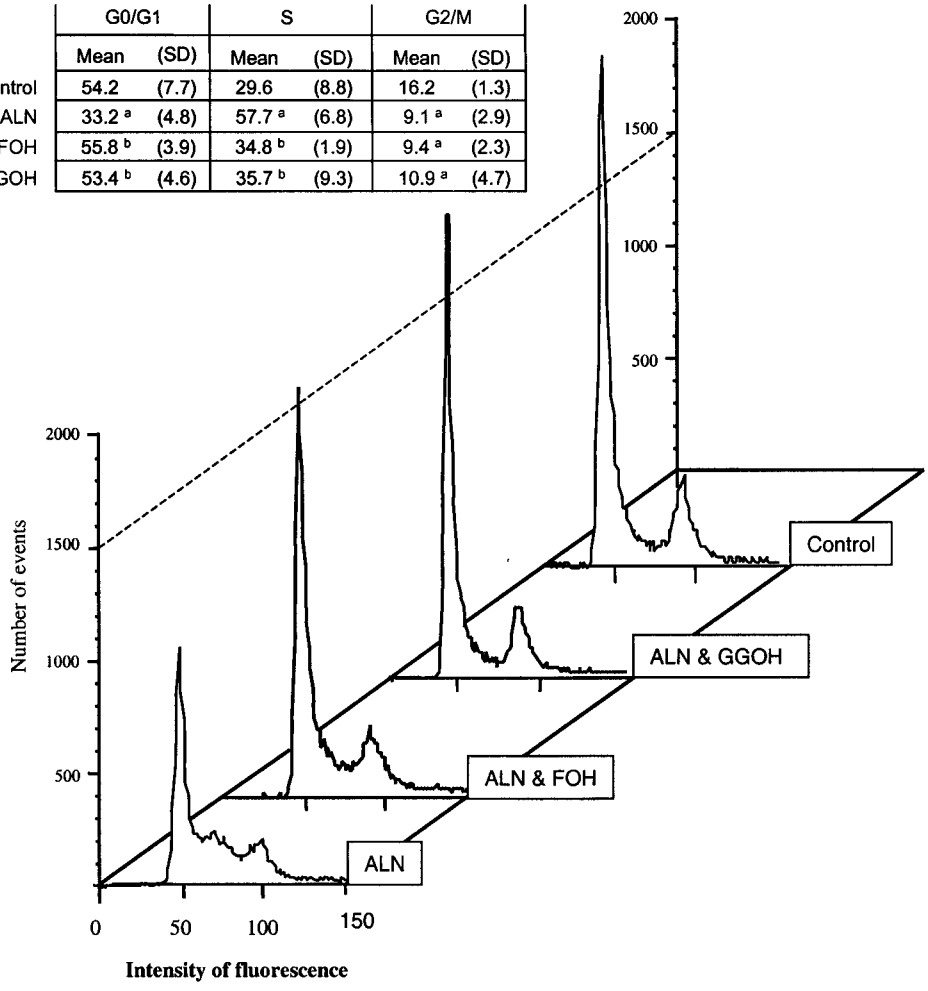

Fig. 4. Distribution of NHEK population in various phases of the cell cycle. NHEKs were treated with indicated compounds in the presence of phosphatidylcholine (40 μg/ml) for 48 h and then fixed, stained with propidium iodide, and 20,000 cells/treatment were analyzed by FACS as described under *Materials and Methods*. Graph shows FACS profile from control NHEKs (top) and cells treated as follows: 30 μM ALN with 10 μM GGOH; 30 μM ALN with 10 μM FOH, and 30 μM ALN. Inset table shows distribution of cells (%) in G_0/G1, S, and G_2/M phases as determined by ModFit LT software. Data are mean percent ± S.D.; $n = 3$. Statistical significance: $^a p < 0.05$ versus ALN; $^b p < 0.01$ versus control.

tum basale likely encounter BP at concentrations lower than those within the lumen after gastric reflux unless local damage exposes the underlying strata. In our model, ALN and RIS suppressed NHEK growth in a dose-dependent manner, beginning at approximately 10% of the concentration found in the stomach or esophageal reflux after clinical dosing. Growth effects were maximal as N-BP concentrations approached the highest clinically relevant dose. The findings suggest that ALN and RIS inhibit NHEK growth primarily by acting on the mevalonate pathway, thus blocking cholesterol synthesis and geranylgeranylation. These conclusions are further supported by the absence of apoptosis and necrosis and by the partial prevention of N-BP-induced effects after restoration of the downstream metabolites geranylgeranyl and farnesyl diphosphates and cholesterol.

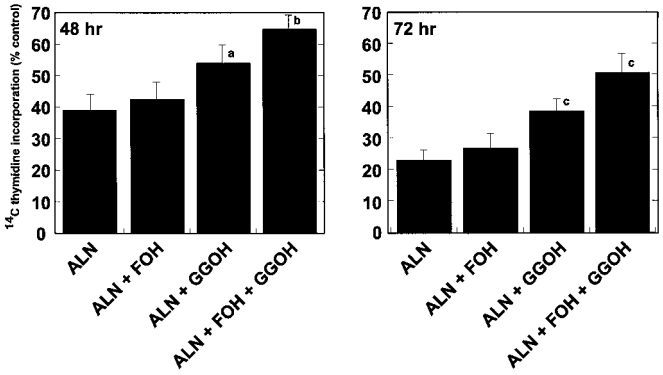

Fig. 5. FOH and GGOH increase ALN-inhibited growth. NHEKs were grown for 72 h in the presence of ALN (30 μM) and in the presence or absence of FOH (10 μM), GGOH (10 μM) or both. [^{14}C]thymidine incorporation was measured at the 48 and 72 h time points as described under *Materials and Methods*. Thymidine incorporation is presented as percentage of growth in the absence of ALN. Data are mean ± S.D. (n = 3 triplicate experiments) $^{a}p < 0.02$, $^{b}p < 0.06$ and $^{c}p < 0.05$ versus ALN alone.

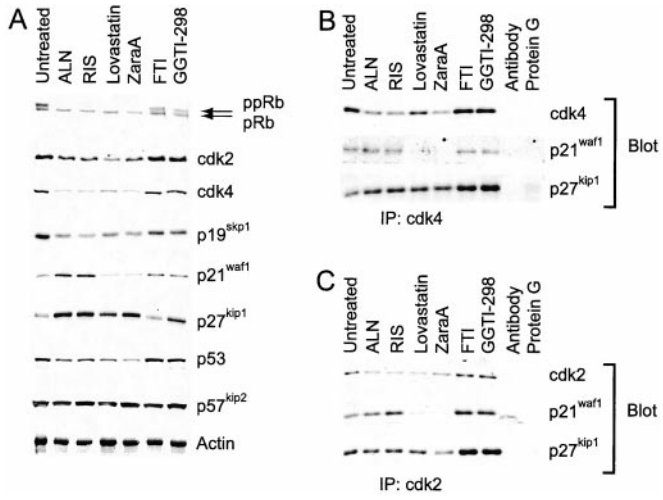

Fig. 6. Effects of N-BPs and other mevalonate pathway and isoprenylation inhibitors on pRb, cdks, and cdk inhibitors. NHEKs were treated for 72 h, as indicated, and then cells were lysed for immunoblot analyses, as described under *Materials and Methods*, of crude lysates (A), anti-cdk4 immunoprecipitates (B), or anti-cdk2 immunoprecipitates (C). Antibodies used to probe immunoblots are indicated at the right of each panel. Treatments are indicated above each lane at the following concentrations: 300 μM ALN, 300 μM RIS, 3 μM LOV, 3 μM Zara-A, 0.3 μM FTI-1, and 3 μM GGTI-298. For immunoprecipitates (B and C), additional controls included anti-cdk antibodies without added lysate ("Antibody") and protein lysate without added antibody ("Protein G"). Data are representative of ≥ 4 independent experiments (n = 2 for p57 immunoblot).

ALN and RIS acted very similarly to each other, and in some respects differently from the other pathway inhibitors used, in inhibiting isoprenylation of Rap1A, hDNAJ, and Ras, consistent with their identical target in the inhibition of the mevalonate pathway, farnesyl diphosphate synthase. Their similar dose response for inhibition of geranylgeranylation and NHEK growth further supports the hypothesis that the observed growth suppression is caused by inhibition of the mevalonate pathway. Accordingly, LOV, the inhibitor of HMG-CoA reductase (upstream in the mevalonate pathway), mimicked the N-BP effects on NHEK growth, consistent with previously described LOV effects on stratified squamous epithelium of the skin. LOV effects on Rap1A geranylgeranylation were comparable with those of the N-BPs; unexpectedly, however, LOV effects on hDNAJ and Ras farnesylation were minimal. The consistent inhibition of geranylgeranylation by N-BP and LOV, minimal effects of the farnesylation inhibitor FTI-1 on NHEK growth, and greater impact of GGOH than FOH on cell growth indicate that geranylgeranylated, more than farnesylated, proteins regulate NHEK growth control.

Preferential isoprenylation effects of LOV are interesting and require further study. Isoprenylation occurs immediately after protein synthesis. The ability of FTI-1 to completely block farnesylation of both hDNAJ and Ras (under similar conditions LOV did not) should rule out the possibility that protein turnover rates were insufficient for detecting LOV inhibition of farnesylation. Isoprenylation inhibition by N-BPs or LOV is indirect, mediated through inhibition of upstream enzymes. Different types of inhibitors may therefore have different effects on the available pools of isoprenylation intermediates. Thus, unlike with GGTI or FTI, measurement of protein isoprenylation in the presence of these agents is useful but cannot be used as a complete measure of the impact of N-BPs or LOV on this metabolic pathway. At any rate, the similar nature of ALN and RIS effects on farnesylation and geranylgeranylation verify that these two N-BPs act via a common mechanism and generate an unique pool of metabolites that is different from that generated by LOV.

Using downstream branch pathway inhibitors we found that Zara-A and GGTI-298 mimicked N-BP effects on NHEK growth to a far greater extent than FTI-1, suggesting again that cholesterol synthesis and geranylgeranylation were more important. Furthermore, the data indicate that N-BP inhibition of cholesterol synthesis and geranylgeranylation have additive effects on growth, although geranylgeranylation seems to play a greater role. In osteoclasts (nonproliferative, terminally differentiated cells), suppression of geranylgeranylation alone was rate-limiting and led to inhibition of bone resorption and induction of apoptosis (Fisher et al., 1999; Reszka et al., 1999; van Beek et al., 1999a). Bergstrom et al. (2000) reported a low incorporation of mevalonate into nonsaponifiable lipids in the osteoclast, possibly because of a sizable pre-existing intracellular pool of cholesterol, which might reduce the impact of N-BPs on this branch pathway.

Effects on binucleation suggested that ALN and RIS, at lower doses, interfered with the late stages of mitosis, primarily cytokinesis. LOV and Zara-A also induced binucleation and accordingly increased the number of cells in G_2/M. The latter was not observed with ALN and RIS, probably because of more prominent effects on earlier phases of the

cell cycle. Comparison of cell cycle and binucleation data suggests that the majority of cells containing 4n DNA may be binucleated (61% for ALN and 88% for RIS versus 13% in controls cells), although aberrant binucleation occurring within the 2n population is possible. The prevention of ALN and Zara-A effects on binucleation by LDL suggest that binucleation was caused primarily by suppression of cholesterol biosynthesis. This is consistent with a previous report that the HMG-CoA reductase inhibitor synvinolin arrests procyclic *Trypanosoma brucei* at cytokinesis (Coppens and Courtoy, 1995).

A second prominent effect produced by N-BPs (at 30 μM) was a reduced transit through S phase observed by FACS analyses. This effect was not seen in NHEKs after treatment with GGTI-298, yet when induced by N-BP was prevented by addition of GGOH, suggesting that inhibition of geranylgeranylation was necessary but not sufficient to generate this effect. FOH also blocked accumulation of NHEKs in S phase but without increasing thymidine incorporation unless GGOH was also added. Partial recovery of thymidine incorporation by added FOH and GGOH could not be further increased by LDL, which reduced thymidine incorporation, especially when added with GGOH. The reason for this remains to be investigated. However, LDL addition reduced binucleation (interference with cytokinesis), a major effect of reduced cholesterol, as indicated by Zara-A treatment. Given that each growth-related phenotype was restored by the relevant metabolites, the preponderance of the evidence suggests that the growth characteristics elicited by N-BP were primarily caused by inhibition of FPP synthase. The S phase may represent the most sensitive point in the cell cycle for N-BP action. Consistent with this conclusion, previous studies have shown that the N-BP incadronate, as well as the HMG-CoA reductase inhibitor mevastatin, arrest myeloma cell growth in S phase, in addition to inducing apoptosis (Shipman et al., 1997; 1998; Aparicio et al., 1998). In other cells, GGTI and LOV arrested in G_1 (Vogt et al., 1997, 1999; Rao et al., 1998, 1999; Naderi et al., 1999), suggesting cell-specific responses. GGOH was consistently more effective than FOH in blocking N-BP or statin effects (Shipman et al., 1998; Vogt et al., 1999). The most profound inhibition of NHEK growth was at 300 μM N-BP, the estimated maximal concentration in the stomach after clinical dosing. FACS analyses suggested that at this concentration the majority of cells were blocked in G_0/G_1. This suggested, and we observed, the hypophosphorylation of pRb, which could block the transition from G_1 to S phase. The subsequent analyses suggest inhibition of pRb phosphorylation via reduction of cdk2 and cdk4 expression coupled to enhanced association with cdk inhibitors, $p21^{waf1}$ and $p27^{kip1}$. This was mimicked by LOV. However, as with isoprenylation, the differences between inhibition of HMG-CoA reductase and FPP synthase were manifest in the profile of cdk inhibition. The N-BPs seemed to enhance uniquely the expression of $p21^{waf1}$ and its binding to cdk4, whereas N-BP and isoprenylation inhibitors enhanced binding to cdk2. In other studies both statins and GGTI-298 increased $p21^{waf1}$ expression or altered association with cdks (Vogt et al., 1997; Lee et al., 1998; Adnane et al., 1998; Rao et al., 1998, 1999). In NHEKs, the profile elicited by LOV and Zara-A were most comparable, which may suggest an enhanced cholesterol-dependent phenotype after treatment with LOV. In most other regards, the cdk profile elicited by the N-BPs was best matched to that of Zara-A and LOV and not to that of GGTI-298 or FTI-1.

In summary, our in vitro findings show N-BP inhibition of NHEK growth, used as a model for the *stratum basale* of the esophagus, caused most likely by inhibition of FPP synthase. The consequent reduction in cholesterol biosynthesis and geranylgeranylation appeared to be rate-limiting. Contrary to N-BP effects on osteoclasts and macrophages (Hughes et al., 1995; Benford et al., 1999; Reszka et al., 1999), there was no induction of apoptosis. ALN and RIS inhibition of NEHK growth occurred at concentrations that can be present in esophageal reflux after clinical dosing. Because there was a striking similarity in the effects of ALN and RIS on all the changes observed, these findings suggest that esophageal irritation caused by these BPs may be mechanism-based. This could apply to effects observed with other N-BPs used in the clinic (e.g., pamidronate, ibandronate, olpadronate) which also inhibit FPP synthase (van Beek et al., 1999b; Bergstrom et al., 2000).

Acknowledgments

We thank Mark Miller and Bohumil Bednar for assistance with FACS analyses.

References

Adnane J, Bizouarn YQ, Qian Y, Hamilton AD and Sebti SM (1998) $p21^{WAF1/CIP1}$ is upregulated by the geranylgeranyltransferase I inhibitor GGTI-298 through a transforming growth factor β- and Sp1-responsive element: Involvement of the small GTPase RhoA. *Mol Cell Biol* **18:**6962–6970.

Amin D, Cornell SA, Gustafson SK, Needle SJ, Ullrich JW, Bilder GE & Perrone MH (1992) Bisphosphonates used for the treatment of bone disorders inhibit squalene synthase and cholesterol biosynthesis. *J Lipid Res* **33:**1657–1663.

Aparicio A, Gardner A, Tu Y, Savage A, Berenson J and Lichtenstein A (1998) In vitro cytoreductive effects on multiple myeloma cells induced by bisphosphonates. *Leukemia* **12:**220–229.

Bai C, Sen P, Hofmann K, Ma L, Goebl M, Harper JW and Elledge S (1996) SKP1 connects cell cycle regulators to the ubiquitin proteolysis machinery through a novel motif, the F-box. *Cell* **86:**263–274.

Benford HL, Frith JC, Auriola S, Monokkonen J and Rogers MJ (1999) Farnesol and geranylgeraniol prevent activation of caspases by aminobisphosphonates: Biochemical evidence for two distinct pharmacological classes of bisphosphonate drugs. *Mol Pharmacol* **56:**131–140.

Bergstrom JE, Bostedor RG, Masarachia PJ, Reszka AA and Rodan GA (2000) Alendronate is a specific, nanomolar inhibitor of farnesyl diphosphate synthase. *Arch Biochem Biophys* **373:**231–241.

Blank MA, Ems BL, Gibson GW, Myers WR, Berman SK, Phipps RJ and Smith PN (1997) Nonclinical model for assessing gastric effects of bisphosphonates. *Dig Dis Sci* **42:**281–288.

Coppens I and Courtoy PJ (1995) Exogenous and endogenous sources of sterols in the culture-adapted procyclic trypomastigotes of Trypanosoma brucei. *Mol Biochem Parasitol* **73:**179–188.

de Groen PC, Lubbe DF, Hirsch LJ, Daifotis A, Stephenson W, Freedholm D, Pryor-Tillotson S, Seleznick MJ, Pinkas H and Wang KK (1996) Esophagitis associated with the use of alendronate. *N Engl J Med* **335:**1016–1021.

Elliott SN, McKnight W, Davies NM, MacNaughton WK and Wallace JL (1998) Alendronate induces gastric injury and delays ulcer healing in rodents. *Life Sci* **62:**77–91.

Feingold KR, Man MQ, Menon GK, Cho SS, Brown BE and Elias PM (1990) Cholesterol synthesis is required for cutaneous barrier function in mice. *J Clin Invest* **865:**1738–1745.

Feingold KR, Man MQ, Proksch E, Menon GK, Brown BE and Elias PM (1991) The lovastatin-treated rodent: A new model of barrier disruption and epidermal hyperplasia. *J Invest Dermatol* **96:**201–209.

Fisher JE, Rogers MJ, Halasy JM, Luckman SP, Hughes DE Masarachia PJ, Wesolowski G Russell‡ RGG Rodan GA and Reszka AA (1999) Alendronate mechanism of action: Geranylgeraniol, an intermediate in the mevalonate pathway, prevents inhibition of osteoclast formation, bone resorption, and kinase activation in vitro. *Proc Natl Acad Sci USA* **96:**133–138.

Hughes DE, Wright KR, Uy HL, Sasaki A, Yoneda T, Roodman GD, Mundy GR and Boyce BF (1995) Bisphosphonates promote apoptosis in murine osteoclasts in vitro and in vivo. *J Bone Miner Res* **10:**1478–1487.

Lee SJ, Mahn JH, Lee J, Nguyen PM, Choi YH, Pirnia F, Kang W-K, Wang X-F, Kim SJ and Trepel JB (1998) Inhibition of the 3-hydroxy-3-methylglutaryl-coenzyme A reductase pathway induces p53-independent transcriptional regulation of $p21^{waf1/cip1}$ in human prostate carcinoma cells. *J Biol Chem* **273:**10618–10623.

Luckman SP, Hughes DE, Coxon FP, Russell RGG and Rogers MJ (1998) Nitrogen-containing bisphosphonates inhibit the mevalonate pathway and prevent post-translational prenylation of GTP-binding proteins, including Ras. *J Bone Miner Res* **13:**581–589.

McGuire TF, Qian Y, Vogt A, Hamilton AD and Sebti SM (1996) Platelet-derived growth factor receptor tyrosine phosphorylation requires protein geranylgeranylation but not farnesylation. *J Biol Chem* **271:**27402–27407.

Menon GK, Feingold KR, Mao Qiang M, Schaude M and Elias PM (1992) Structural basis for the barrier abnormality following inhibition of HMG CoA reductase in murine epidermis. *J Invest Dermatol* **98:**209–219.

Miquel K, Pradines A, Terce F, Selmi S and Favre G (1998) Competitive inhibition of choline phosphotransferase by geranylgeraniol and farnesol inhibits phosphatidylcholine synthesis and induces apoptosis in human lung adenocarcinoma A549 cells. *J Biol Chem* **273:**26179–26186.

Naderi S, Blomhoff R, Myklebust J, Smeland EB, Erikstein B, Norum KR and Blomhoff HK (1999) Lovastatin inhibits G1/S transition of normal human B-lymphocytes independent of apoptosis. *Exp Cell Res* **252:**144–153.

Peter CP, Handt LK and Smith SM (1998a) Esophageal irritation due to alendronate sodium tablets: Possible mechanisms. *Digest Dis Sci* **43:**1998–2002.

Peter CP, Kindt MV and Majka JA (1998b) Comparative study of potential for bisphosphonates to damage gastric mucosa of rats. *Digest Dis Sci* **43:**1009–1015.

Rao S, Lowe M, Herliczek TW and Keyomarsi K (1998) Lovastatin mediated G1 arrest in normal and tumor breast cells is through inhibition of CDK2 activity and redistribution of p21 and p27, independent of p53. *Oncogene* **17:**2393–2402.

Rao S, Porter DC, Chen X, Herliczek T, Lowe M and Keyomarsi K (1999) Lovastatin-mediated G1 arrest is through inhibition of the proteasome, independent of hydroxymethyl glutaryl-CoA reductase. *Proc Natl Acad Sci USA* **96:**7797–7802.

Reszka AA, Halasy-Nagy JM, Masarachia PJ and Rodan GA (1999) Bisphosphonates act directly on the osteoclast to induce caspase cleavage of mst1 kinase during apoptosis. A link between inhibition of the mevalonate pathway and regulation of an apoptosis-promoting kinase. *J Biol Chem* **274:**34967–34973.

Shipman CM, Croucher PI, Russell RG, Helfrich MH and Rogers MJ (1998) The bisphosphonate incadronate (YM175) causes apoptosis of human myeloma cells in vitro by inhibiting the mevalonate pathway. *Cancer Res* **58:**5294–5297.

Shipman CM, Rogers MJ, Apperley JF, Russell RG and Croucher PI (1997) Bisphosphonates induce apoptosis in human myeloma cell lines: A novel anti-tumour activity. *Br J Haematol* **98:**665–672.

Sun J, Qian Y, Chen Z, Marfurt J, Hamilton AD and Sebti SM (1999) The geranylgeranyltransferase I inhibitor GGTI-298 induces hypophosphorylation of retinoblastoma and partner switching of cyclin-dependent kinase inhibitors. A potential mechanism for GGTI-298 antitumor activity. *J Biol Chem* **274:**6930–6934.

Tobert JA (1988) Efficacy and long-term adverse effect pattern of lovastatin. *Am J Cardiol* **11:**28J–34J.

van Beek E, Lowik C, van der Pluijm G and Papapoulos S (1999a) The role of geranylgeranylation in bone resorption and its suppression by bisphosphonates in fetal bone explants in vitro: A clue to the mechanism of action of nitrogen-containing bisphosphonates. *J Bone Miner Res* **14:**722–729.

van Beek E, Pieterman E, Cohen L, Lowik C and Papapoulos S (1999b) Farnesyl pyrophosphate synthase is the molecular target of nitrogen-containing bisphosphonates. *Biochem Biophys Res Commun* **264:**108–111.

Vogt A, Sun J, Qian Y, Hamilton AD and Sebti SM (1997) The geranylgeranyltransferase-I inhibitor GGTI-298 arrests human tumor cells in G0/G1 and induces $p21^{WAF1/CIP1/SDI1}$ in a p53-independent manner. *J Biol Chem* **272:**27224–27229.

Vogt A, Qian Y, McGuire TF, Hamilton AD and Sebti SM (1999) Protein geranylgeranylation, not farnesylation, is required for the G1 to S phase transition in mouse fibroblasts. *Oncogene* **13:**1991–1999.

Wallace JL, Dicay M, Mcknight W, Bastaki S and Blank MA (1999) N-bisphosphonates cause gastric epithelial injury independent of effects on the microcirculation. *Aliment Pharmacol Ther* **13:**1675–1682.

Williams TM, Bergman JM, Brashear K, Breslin MJ, Dinsmore CJ, Hutchinson JH, MacTough SC, Stump CA, Wei DD, Zartman CB, Bogusky MJ, Culberson JC, Buser Doepner C, Davide J, Greenberg IB, Hamilton KA, Koblan KS, Kohl NE, Liu DM, Lobell RB, Mosser SD, O'Neill TJ, Rands E, Schaber MD, Wilson F, Senderak E, Motzel SL, Gibbs JB, Graham SL, Heimbrook DC, Hartman GD, Oliff AI and Huff JR (1999) N-arylpiperazinone inhibitors of farnesyltransferase: Discovery and biological activity. *J Med Chem;* **42:**3779–3784.

Yu Z-K, Gervais JL and Zhang H (1999) Human CUL-1 associates with the SKP1/SKP2 complex and regulates p21(CIP1/WAF1) and cyclin D proteins. *Proc Natl Acad Sci USA* **95:**11324–11329.

Send reprint requests to: Dr. Alfred A. Reszka, Department of Bone Biology, WP26A-1000, Merck Research Laboratories, West Point, PA, 19486. E-mail: alfred_reszka@merck.com